

# CAPTURE REACTIONS OF ASTROPHYSICAL INTEREST IN THE SHELL MODEL EMBEDDED IN THE CONTINUUM\* \*\*

K. BENNACEUR <sup>a</sup>, F. NOWACKI <sup>b</sup>, J. OKOŁOWICZ <sup>a,c</sup>  
AND M. PŁOSZAJCZAK <sup>a</sup>

<sup>a</sup> Grand Accélérateur National d'Ions Lourds (GANIL)  
CEA/DSM-CNRS/IN2P3, BP 5027, F-14076 Caen Cedex 05, France

<sup>b</sup> Laboratoire de Physique Théorique Strasbourg (EP 106)  
3-5 rue de l'Université, F-67084 Strasbourg Cedex, France

<sup>c</sup> Institute of Nuclear Physics  
Radzikowskiego 152, 31-342 Kraków, Poland

*(Received November 20, 1999)*

We apply the realistic shell model which includes the coupling between many-particle (quasi-)bound states and the continuum of one-particle scattering states, to the spectroscopy of mirror nuclei as well as to the description of low energy cross section in the capture reactions.

PACS numbers: 21.60.Cs, 24.10.Eq, 25.40.Lw, 27.20.+n

## 1. Introduction

50 years have passed since the introduction the Shell Model (SM) [1]. Its foundations have been understood when the connection between elementary nucleon-nucleon interaction and the existence of a smooth effective nuclear potential with the spin-orbit coupling was established [2]. The investigation of how the residual two-body interaction acting between nucleons in this effective nuclear potential can give rise to the observed spectra, started in mid 50s with the first application of the multiconfigurational SM in  $p$ -shell, aiming at an understanding of the evolution of nucleon coupling scheme from  $LS$  toward  $jj$  coupling with increasing mass number [3,4]. These works have given birth to the nuclear structure theory which is flourishing nowadays and whose breath taking achievements accompany the recent experimental

---

\* Invited talk presented at the XXVI Mazurian Lakes School of Physics, Krzyże, Poland, September 1-11, 1999.

\*\* This lecture is devoted to the memory of late Professor Zdzisław Szymański.

efforts trying to reach drip-lines and testing limits of nuclear stability at high angular momenta and extreme shapes.

At the beginning, the scattering continuum was absent in the SM. The nucleons were assumed to occupy the single particle (s.p.) orbits of bound average potential, perfectly isolated from the external environment of scattering states. The success of SM was so convincing that even problems encountered early in describing the spectra of mirror nuclei (*e.g.*  $^{13}\text{C}$ ,  $^{13}\text{N}$  [5]), which revealed a subtle influence of continuum depending on the position of respective particle emission thresholds, did not change the fundamental separation of the ‘*nuclear structure*’ and the ‘*nuclear reaction*’ methods. This separation, which grew with time to a kind of paradigm of nuclear physics, was weaker in early days. It was Feshbach at the end of 50s who expressed the collision matrix of optical model in terms of matrix elements of the nuclear Hamiltonian [6]. This has given strong push to the SM approach to the nuclear reactions [7]. The basic idea of this continuum shell model (CSM) approach is to use the finite depth s.p. potential and to consider no more than one nucleon in the scattering state [8]. The latter limitation restricts the applicability of the CSM to reaction involving one nucleon in the continuum.

Description of weakly bound exotic nuclei close to the drip-lines such as, *e.g.*,  $^8\text{B}$  or  $^{11}\text{Li}$  in their ground state (g.s.), is an exciting theoretical challenge. The proximity of particle continuum in these nuclei imply that virtual excitations to continuum states cannot be neglected as they modify the effective interactions and cause the large spatial extension of density distribution (nuclear halo effect). The Shell Model Embedded in the Continuum (SMEC), in which *realistic*  $N$ -particle SM solutions for (quasi-)bound states are coupled by the residual interaction to the one-particle scattering continuum, is a recent development of the CSM [9] for the description of complicated low energy excitations of weakly bound nuclei.

## 2. Few remarks on Shell Model Embedded in the Continuum

In SMEC, the bound (interior) states together with its environment of one-nucleon channels form a closed quantum system. Using the projection operator technique, one separates the  $P$  subspace of asymptotic channels from the  $Q$  subspace of many-body localized states which are build up by the bound s.p. wave functions and by the s.p. resonance wave functions.  $P$  subspace is assumed to contain  $(N - 1)$ -particle states with nucleons on bound s.p. orbits and one nucleon in the scattering state. Also the s.p. resonance wave functions outside of the cutoff radius  $R_{\text{cut}}$  are included in the  $P$  subspace. The resonance wave functions for  $r < R_{\text{cut}}$  are included in the  $Q$  subspace. The wave functions in  $Q$  and  $P$  are then properly renormalized

in order to ensure the orthogonality of wave functions in both subspaces.

The discussion of SMEC formalism can be found in Ref. [10, 11]. The complete solution in SMEC is constructed in three steps. In the first step, one calculates the (quasi-) bound many-body states in  $Q$  subspace by solving the multiconfigurational SM problem:  $H_{QQ}\Phi_i = E_i\Phi_i$ , where  $H_{QQ}$  is the SM effective Hamiltonian which is appropriate for the SM configuration space used. To generate both the radial s.p. wave functions in the  $Q$  subspace and the scattering wave functions in  $P$  subspace we use the average potential of Saxon–Woods (SW) type with the spin–orbit and Coulomb potentials included [10, 11]. For the continuum part, one solves the coupled channel equations:

$$\sum_{c'} (E^{(+)} - H_{cc'}) \xi_E^{c'(+)} = 0, \quad (1)$$

where index  $c$  denotes different channels and the superscript  $(+)$  means that boundary conditions for incoming wave in the channel  $c$  and outgoing scattering waves in all channels are used. The channel states are defined by coupling of one nucleon in the scattering continuum to the many-body SM state in  $(N - 1)$ -nucleus. Finally, the third system of equations consists of inhomogeneous coupled channel equations with the source term which couples the  $N$ -nucleon localized SM states with  $(N - 1)$ -nucleon localized SMEC states plus one nucleon in the continuum. These equations define functions  $\omega_i^{(+)}$ , which describe the decay of quasi-bound state  $\Phi_i$  in the continuum.

Using the SM Hamiltonian in  $Q$  subspace implies that the coupling between (quasi-) bound and scattering states has to be generated by the residual interaction (for that purpose we use the zero-range interaction with the spin-exchange included). The matrix elements of this interaction enter both in the source term of inhomogeneous coupled channel equations and in the channel–channel coupling potential (1):  $H_{cc'} = (T + U)\delta_{cc'} + v_{cc'}^J$ , where  $T$  is the kinetic energy operator and  $v_{cc'}^J$  is the coupling generated by the residual interaction. The potential for channel  $c$  consists of “initial guess”,  $U(r)$ , and diagonal part of coupling potential  $v_{cc}^J$  which depends on both the s.p. orbit  $\phi_{l,j}$  and the considered many-body state  $J^\pi$ . This modification of the initial potential  $U(r)$  change the generated s.p. wave functions  $\phi_{l,j}$  defining  $Q$  subspace, which in turn modify the diagonal part of the residual force, the source term, *etc.* Hence, the solution of coupled channel equations (1) is accompanied by the self-consistent iterative procedure which, for each channel independently, yields the corresponding self-consistent potential:  $U^{(\text{sc})}(r) = U(r) + v_{cc}^{J(\text{sc})}(r)$ , and consistent with it the renormalized matrix elements of coupling force. The parameters of  $U(r)$  are chosen in

such a way that  $U^{(\text{sc})}(r)$  reproduces energies of experimental s.p. states, whenever their identification is possible.

### 3. Example of applications: ${}^8\text{Li}$ , ${}^8\text{B}$

The solution of solar neutrino problem, *i.e.*, an observed deficit of neutrinos with respect to predictions of the Standard Solar Model (SSM) [12], is passing through an understanding of the capture reaction:  ${}^7\text{Be}(p, \gamma){}^8\text{B}$ . ( ${}^8\text{B}$  produced in the solar interior is the principal source of high energy neutrinos detected in solar neutrino experiments.) At the solar energies ( $E_{\text{CM}} \sim 20 \text{ keV}$ ), this cross-section is too small to be directly measurable. For this reason, the theoretical analysis of this reaction is so important. On the other hand, whenever measurement is feasible ( $> 150 \text{ keV}$ ), the exact value of the capture cross section depends: (*i*) on the normalization obtained indirectly from the  ${}^7\text{Li}(d, p){}^8\text{Li}$  cross section and, (*ii*) on the model dependent extrapolation of measured values of the cross-section down to the interesting domain of solar energies. Measured values for  ${}^7\text{Be}(p, \gamma){}^8\text{B}$  cross section are varying strongly, though recent experiments consistently indicate low values ( $S < 20 \text{ eV}\cdot\text{b}$ ) of the astrophysical factor  $S \equiv \sigma_{\text{CM}}(E_{\text{CM}})E_{\text{CM}} \exp(-2\pi\eta)$ , where  $\eta = e^2 Z_1 Z_2 / \hbar v$  [13, 14].

Part of the theoretical ambiguities can be removed by a simultaneous study of the  ${}^7\text{Li}(n, \gamma){}^8\text{Li}$  mirror reaction, which has also been studied by several experimental groups [15]. In the context of the solar neutrino problem, the  ${}^7\text{Li}(n, \gamma){}^8\text{Li}$  cross section is often used to extrapolate the  ${}^7\text{Be}(p, \gamma){}^8\text{B}$  cross section down to the solar energies [13]. The  ${}^7\text{Li}(n, \gamma){}^8\text{Li}$  reaction at very low energies is also extremely interesting in itself as it provides the essential element of rapid process of primordial nucleosynthesis of nuclei with  $A \geq 12$  in the inhomogeneous big-bang models [16] allowing to bridge the gap of mass  $A = 8$  and to produce heavy elements.

#### 3.1. The self-consistent determination of $Q$ subspace

Construction of  $Q$  subspace by the SMEC with the SM source implies that the self-consistent s.p. potential  $U^{(\text{sc})}(r)$  depends on the s.p. wave function  $\phi_{l,j}$ , the total spin  $J$  of the  $N$ -nucleon system as well as on the one-body matrix elements of  $(N-1)$ -nucleon daughter system. In the studied cases of  ${}^8\text{B}$ ,  ${}^8\text{Li}$ , all these potentials have the same parameters of radius  $R_0 = 2.4 \text{ fm}$ , surface diffuseness  $a = 0.52 \text{ fm}$ , and spin-orbit coupling  $V_{\text{SO}} = -4 \text{ MeV}$ . Cohen-Kurath (CK) interaction [17] is used as a SM interaction and the strength of the residual interaction is:  $V_{12}^{(0)} = 650 \text{ MeV}\cdot\text{fm}^3$  [10]. Fig. 1 shows typical examples of potentials in  ${}^8\text{B}$ , here for the proton s.p. orbital  $0p_{3/2}$ , in two different total spin states:  $J^\pi = 1^+, 2^+$ . The same initial

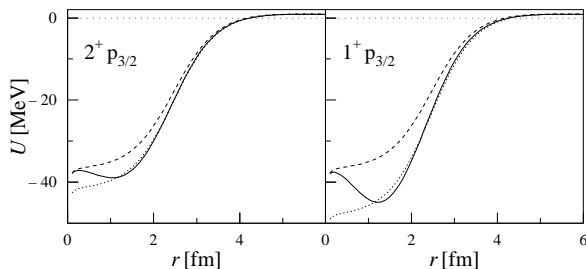


Fig. 1. Example of finite-depth s.p. potentials for  $0p_{3/2}$  radial s.p. wave functions in  $J^\pi = 1^+, 2^+$  ( $T = 1$ ) bound states and resonances of  ${}^8\text{B}$  [10]. Different curves denote: the initial potential  $U(r)$  (the dashed line), the self-consistent potential  $U^{(\text{sc})}(r)$  (the solid line), and the equivalent potential  $U^{(\text{eq})}(r)$  of the SW type which yields the proton  $0p_{3/2}$  orbit at the same energy as in the self-consistent potential.

potential  $U(r)$  is taken both for  $2^+$  and  $1^+$  states. The spectroscopic factor of proton  $0p_{3/2}$  s.p. state in the g.s. is close to 1 [17]. This allows to identify position of proton  $0p_{3/2}$  s.p. orbit in  $J^\pi = 2^+$  state, *i.e.*, we demand that  $U^{(\text{sc})}(r)$  provides  $0p_{3/2}$  s.p. state at  $-137\text{keV}$ , corresponding to the binding energy of the  $2_1^+$  g.s. in  ${}^8\text{B}$ .

$U^{(\text{sc})}$  exhibits for small  $r$  a clear maximum which is absent in  $U(r)$ . The self-consistent potentials  $U^{(\text{sc})}(2^+)$  and  $U^{(\text{sc})}(1^+)$  are different, in spite of the fact that the initial potential  $U(r)$  is the same in both cases. The dotted lines in Fig. 1 show the equivalent s.p. average potentials  $U^{(\text{eq})}(r)$ . For the same SW parameterization as in  $U(r)$ , the depth parameter is adjusted in  $U^{(\text{eq})}(r)$  to reproduce the energy of  $0p_{3/2}$  s.p. orbit in  $U^{(\text{sc})}(r)$ . Clearly,  $U^{(\text{eq})}(r)$  and  $U^{(\text{sc})}(r)$  differ strongly in the potential interior. On the contrary, the surface region shows in general weak sensitivity to the self-consistent correction, except for weakly-bound many-body states having an important admixture of  $l = 0$  and  $l = 1$  neutron s.p. states.

There is no clear indication concerning the position of proton  $0p_{1/2}$  s.p. orbit. Using the same  $U(r)$  as used to determine  $U^{(\text{sc})}(r)$  for  $0p_{3/2}$  s.p. state, we get the  $0p_{1/2}$  proton s.p. orbit in  $U^{(\text{sc})}(r)$  at  $\varepsilon_{p_{1/2}} = +0.731\text{MeV}$  in  $J^\pi = 2^+$  states and at  $\varepsilon_{p_{1/2}} = +0.311\text{MeV}$  in  $J^\pi = 1^+$  states. Consequently, the energy splitting of  $p_{3/2}$  and  $p_{1/2}$  orbitals is also state dependent.

Many spectroscopic observables have been calculated for  ${}^8\text{B}$  and  ${}^8\text{Li}$  [10]. The quadrupole moment  $\langle Q \rangle$  of  ${}^8\text{B}$  provides a useful test of the SMEC wave function, in particular of its radial part. The SMEC solutions yields:  $\langle Q \rangle_{\text{th}} = 6.99\text{e fm}^2$ , in good agreement with the experimental value [18]:

$\langle Q \rangle_{\text{exp}} = 6.83 \pm 0.21 \text{ e fm}^2$ . This theoretical value has been obtained assuming the effective charges:  $e_p = 1.35$ ,  $e_n = 0.35$ , and the SM spectroscopic factors for the CK interaction. The analogous calculation in  ${}^8\text{Li}$  yields:  $\langle Q \rangle_{\text{th}} = 2.78 \text{ e fm}^2$ , close to the experimental value [18]:  $\langle Q \rangle_{\text{exp}} = 3.27 \pm 0.06 \text{ e fm}^2$ .

### 3.2. Radiative capture cross-sections

Once the parameters of the initial SW potential and the residual interaction coupling states in  $Q$  and  $P$  have been fixed based on the structural informations, we calculate the capture cross-section for  ${}^7\text{Be}(p, \gamma){}^8\text{B}$  (see Fig. 2). We found that the  $E1$  and  $E2$  contributions as well as the total cross-section are insensitive to the size of spin-exchange term in the residual force. On the contrary, the  $M1$  contribution and particularly its resonant part, are sensitive to it. Hence, the Coulomb dissociation (CD) experiments, in which the contributions of  $E2$  and  $M1$  multipolarities as well as nuclear breakup can be disproportionately enhanced in certain kinematical regimes will hopefully give some information about the continuum coupling [19]. The low energy dependence of  $S(E)$  (see Fig. 2) can be fitted by:  $S(E) = S(0) \exp(\hat{\alpha}E + \hat{\beta}E^2)$ . In the range of c.m. energies up to 100 keV the fit yields:  $S(0) = 19.594 \text{ eV}\cdot\text{b}$ ,  $\hat{\alpha} = -1.544 \text{ MeV}^{-1}$ ,  $\hat{\beta} = 6.468 \text{ MeV}^{-2}$ .

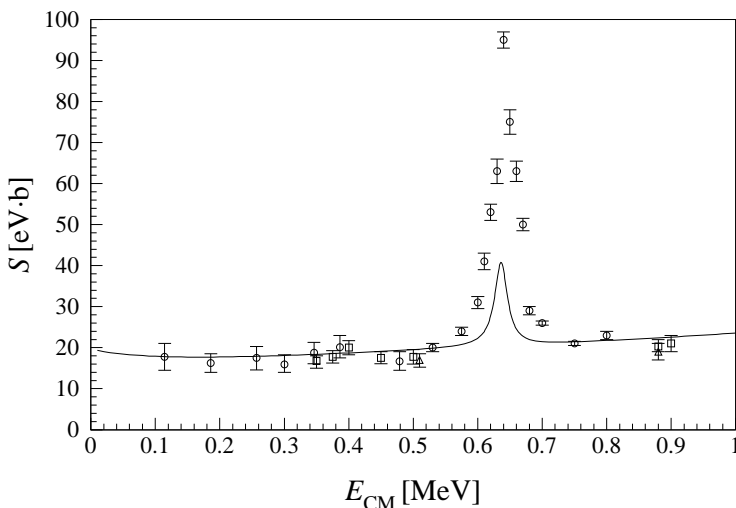


Fig. 2. The astrophysical  $S$ -factor for the reaction  ${}^7\text{Be}(p, \gamma){}^8\text{B}$  is plotted as a function of c.m. energy. The SMEC calculations have been done using the spin-exchange parameter 0.05 [10]. The experimental points are from Refs. [13, 14].

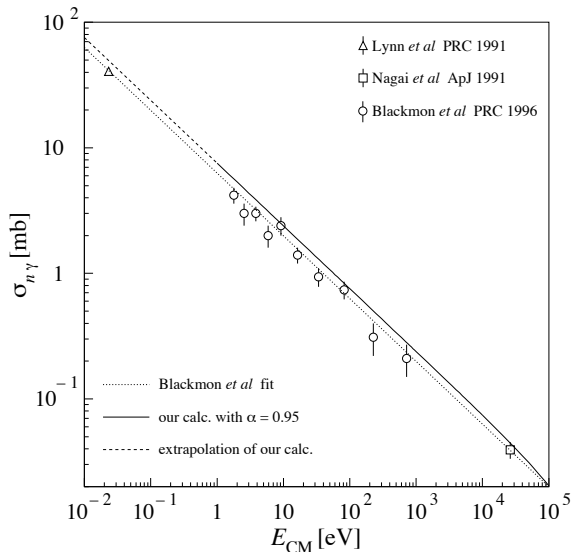


Fig. 3. The cross-section for the reaction  ${}^7\text{Li}(n, \gamma){}^8\text{Li}$  is plotted as a function of c.m. energy. The experimental points are taken from [15].

The mirror reaction:  ${}^7\text{Li}(n, \gamma){}^8\text{Li}$  together with a simultaneous description of energy spectra and particle decay widths of  ${}^8\text{B}$  and  ${}^8\text{Li}$ , provides a stringent test for SMEC calculations. The SM interaction and SM many-body wave functions (*e.g.* the spectroscopic amplitudes) are identical in both cases. The self-consistent one-body potentials which take into account residual coupling of  $Q$  and  $P$  subspaces and which determine the radial formfactors of s.p. wave functions used in the calculation of matrix elements of the residual interaction, are optimized in the same way in  ${}^8\text{B}$  and in  ${}^8\text{Li}$ . Finally, the parameters of direct and spin-exchange terms in the residual interaction are also the same, so the modification of coupling matrix elements in  ${}^8\text{B}$  and  ${}^8\text{Li}$  is solely due to the different radial shape of s.p. wave functions in the corresponding self-consistent potentials for different  $J^\pi$  of many-body states. In the case of neutrons, the collision integral is sensitive to the nuclear interior even in the low energy limit. The scattering lengths  $a_S$ , where  $S$  is the channel spin, are known from elastic scattering of neutrons. So for the  $s$ -wave in the initial channel we use a procedure of readjustment of appropriate  $s$ -wave scattering potentials in order to reproduce experimental values of scattering lengths [20]. Fig. 3 shows the total neutron capture cross-section as a function of the c.m. energy. The SMEC calculation reproduces very well the experimental data at these very low energies.

### 3.3. Coulomb dissociation cross section

The CD method provides an alternative indirect way to determine the cross sections for the radiative capture reactions at low energies. The double differential cross-section for the Coulomb excitation of  ${}^8\text{B}$  from its g.s. to the continuum, with a definite multipolarity of order  $\pi\lambda$  is given by [21]:

$$\frac{d^2\sigma}{d\Omega_{8_{B^*}}dE_{\text{CM}}} = \sum_{\pi\lambda} \frac{1}{E_{\text{CM}}} \frac{dn_{\pi\lambda}}{d\Omega_{8_{B^*}}} \sigma_{\gamma}^{\pi\lambda}(E_{\gamma}), \quad (2)$$

In Eq. (2),  $\Omega_{8_{B^*}}$  defines the direction of the c.m. of the [ $p - {}^7\text{Be}$ ] system (to be referred as  ${}^8\text{B}^*$ ) with respect to the beam direction.  $\sigma_{\gamma}^{\pi\lambda}(E_{\gamma})$  is the cross-section for the photo-disintegration process:  $\gamma + {}^8\text{B} \rightarrow {}^7\text{Be} + p$ , with photon energy  $E_{\gamma}$ , and multipolarity  $\pi = \text{E}$  (electric) or  $\text{M}$  (magnetic), and order  $\lambda = 1, 2, \dots$ , which is related to that of the radiative capture process:  ${}^7\text{Be} + p \rightarrow {}^8\text{B} + \gamma$ , through the theorem of detailed balance.  $E_{\gamma}$  is given by  $E_{\text{CM}} = E_{\gamma} + Q$ , with  $Q = 0.137$  MeV. In most cases, only one or two multipolarities dominate the radiative capture as well as the Coulomb dissociation cross sections.  $n_{\pi\lambda}(E_{\gamma})$  in Eq. (2) represents the number of equivalent (virtual) photons provided by the Coulomb field of the target to the projectile [22].

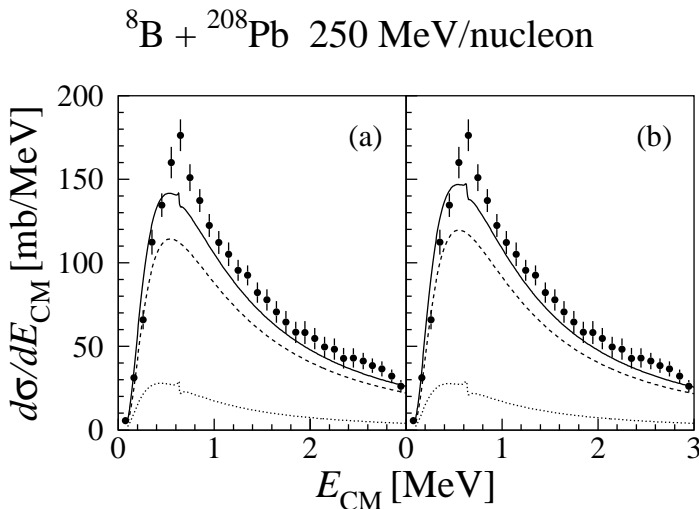


Fig. 4. Comparison of the  $E1 + E2$  (solid lines) CD cross sections calculated for the two versions of SMEC for different amount of the spin-exchange [19] with the experimental data [23]. The individual  $E1$  and  $E2$  components are shown by dashed and dotted lines respectively.

In Fig. 4, we present the comparison of the measured CD cross sections for the reaction  ${}^8\text{B} + {}^{208}\text{Pb} \rightarrow {}^8\text{B}^* + {}^{208}\text{Pb}$  at  $E/A = 250\text{MeV}$  [23], with those calculated for two different input capture cross sections of SMEC, which differ by the amount of the spin-exchange. In (a) the spin-exchange parameter equals 0.27 and in (b) it equals 0.05. The latter case corresponds to an almost pure Wigner force limit for this coupling. The CD data at these high energies seem to show sensitivity to the capture cross sections, in particular to its M1 and E2 components, calculated within different models of  ${}^8\text{B}$  structure. We would like to recall that at lower beam energies (*e.g.*, the RIKEN experiments [24]), the contribution of M1 multipolarity was almost negligible. On the other hand, one can see from Fig. 4, where we show the CD calculations for only E1 (dashed lines) and E2 (dotted lines) multiplicities and their sum (solid line) that it is not possible to explain the data in the region of  $E_{\text{CM}}$  between 500–750 keV without the contribution of the M1 multipolarity. This sensitivity of the higher energy breakup data to the M1 multipolarity makes it possible to use this to supplement the information on the continuum structure of  ${}^8\text{B}$  which was not feasible by similar studies at lower beam energies.

#### 4. Conclusions

We have shown here few selected applications of the SMEC, which is a natural extension of the SM for the study of both nuclear structure and nuclear reactions for weakly bound nuclei. The coherent treatment of the  $Q$  and  $P$  subspaces allows to cross-check the effective interactions both on the structure data and the reaction data. This allows for a fruitful reexamination of the SM effective interactions for nuclei far from the  $\beta$ -stability line. Moreover, reaction data can be used to gain further information about the effective interactions by analyzing the  $N$ -body nature of resonances. SMEC model in its present form includes the coupling to one-nucleon continuum. The wealth of experimental data can be described in a unified framework of SMEC. These include: (i) the calculation of energy spectra,  $B(\Pi\lambda)$  transition matrix elements and various static nuclear moments such as the magnetic or mass/charge quadrupole moments *etc.*, (ii) the calculation of various radiative capture processes:  $(p, \gamma)$ ,  $(n, \gamma)$ , Coulomb breakup processes:  $(\gamma, p)$ ,  $(\gamma, n)$  and elastic or inelastic cross sections  $(p, p')$ ,  $(n, n')$ ; some of these observables have been discussed in this work. Problem of isospin symmetry breaking due to the coupling to the continuum can be addressed by comparing electromagnetic processes, *e.g.*,  $B(\Pi\lambda)$  transition matrix elements for certain states in mirror nuclei, and weak interaction processes like the first-forbidden  $\beta$ -decay in mirror reactions. Finally, for nuclei close and beyond the proton (neutron) drip lines, the spontaneous

proton (neutron) radioactivity can be studied in the microscopic framework of SMEC (SM). These unifying features of SMEC approach are extremely useful for understanding of the structure of exotic nuclei far from the  $\beta$ -stability for which the available experimental information will be scarce.

Complicated resonance structures play vital role in the near threshold behaviour of various capture processes involved in the stellar nucleosynthesis. We have shown some results for mirror reactions:  ${}^7\text{Be}(p, \gamma){}^8\text{B}$  and  ${}^7\text{Li}(n, \gamma){}^8\text{Li}$ . Further applications to  ${}^{16}\text{O}(p, \gamma){}^{17}\text{F}$  can be found in [11]. Other important reactions of CNO-cycles, like:  ${}^{13}\text{N}(p, \gamma){}^{14}\text{O}$ ,  ${}^{17}\text{F}(p, \gamma){}^{18}\text{Ne}$ ,  ${}^{19}\text{Ne}(p, \gamma){}^{20}\text{Na}$  or  ${}^{21}\text{Ne}(p, \gamma){}^{22}\text{Na}$  are presently under the investigation (for further discussion see [25]). The SMEC can be easily extended also for the description of  $\nu$ -nucleosynthesis [25,26]. More complicated decay channels involving, *e.g.*,  $\alpha$  particle,  ${}^3\text{He}$  or  ${}^3\text{H}$  in the continuum, are beyond the scope of SMEC in its present form, though future extension of the SMEC for such cluster configurations is possible in a framework proposed by Balashov *et al.* [27].

It is a pleasure to acknowledge stimulating discussions with E. Caurier, S. Drożdż, I Rotter and R. Shyam at various stages of the development of this project. This work was partly supported by KBN Grant No. 2 P03B 097 16 and the Grant No. 76044 of the French–Polish Cooperation.

## REFERENCES

- [1] O. Haxel, J.H.D. Jensen, H.E. Suess, *Phys. Rev.* **75**, 1766 (1949); M.G. Mayer, *Phys. Rev.* **78**, 16 (1950).
- [2] K.A. Brueckner, in D.R. Bates, *Quantum Theory*, Vol. III, Chapt. VIII, Academic Press, New, York, London 1962; K.A. Brueckner, L. Gammel, *Phys. Rev.* **109**, 1023 (1958); H.A. Bethe, *Phys. Rev.* **103**, 1353 (1956).
- [3] A.M. Lane, *Proc. Phys. Soc. A* **68**, 189 (1955); *Proc. Phys. Soc. A* **68**, 197 (1955); D. Kurath, *Phys. Rev.* **101**, 216 (1956).
- [4] D.H. Wilkinson, Proc. Robert A. Welsh Foundation Conf. Chemical Research. I. The Structure of the Nucleus, Houston, Texas 1957, p. 13.
- [5] J.B. Ehrman, *Phys. Rev.* **81**, 412 (1951).
- [6] H. Feshbach, *Ann. Phys.* **5**, 357 (1958); *Ann. Phys.* **19**, 287 (1962).
- [7] W. Brenig, *Nucl. Phys.* **13**, 333 (1959); U. Fano, *Phys. Rev.* **124**, 1866 (1961); L.S. Rodberg, *Phys. Rev.* **124**, 210 (1961); W.M. Macdonald, *Nucl. Phys.* **54**, 393(1964); *Nucl. Phys.* **56**, 636 (1964).
- [8] C. Mahaux, H. Weidenmüller, *Shell-Model Approach to Nuclear Reactions*, North-Holland, Amsterdam 1969.
- [9] H.W. Bartz, I. Rotter, J. Höhn, *Nucl. Phys.* **A275**, 111 (1977); *Nucl. Phys.* **A307**, 285 (1977).

- [10] K. Bennaceur, F. Nowacki, J. Okołowicz, M. Płoszajczak, *J. Phys. G* **24**, 1631 (1998); *Nucl. Phys.* **A651**, 289 (1999).
- [11] K. Bennaceur, F. Nowacki, J. Okołowicz, M. Płoszajczak, Preprint GANIL P 99/26.
- [12] J.N. Bahcall, R.K. Ulrich, *Rev. Mod. Phys.* **60**, 297 (1988).
- [13] B.W. Filippone *et al.*, *Phys. Rev. Lett.* **50**, 452 (1983).
- [14] F. Hammache *et al.*, *Phys. Rev. Lett.* **80**, 928 (1998).
- [15] Y. Nagai *et al.*, *Ap. J.* **381**, 444 (1991); J.E. Lynn, E.T. Jurney, S. Raman, *Phys. Rev.* **C44**, 764 (1991); J.C. Blackman *et al.*, *Phys. Rev.* **C54**, 383 (1996).
- [16] J.H. Applegate, C.J. Hogan, R.J. Scherrer, *Phys. Rev.* **D35**, 1151 (1987); *Ap. J.* **329**, 572 (1988); G.M. Fuller, G.J. Mathews, C.R. Alcock, *Phys. Rev.* **D37**, 1380 (1988).
- [17] S. Cohen, D. Kurath, *Nucl. Phys.* **A73**, 1 (1965).
- [18] T. Minamisono *et al.*, *Phys. Rev. Lett.* **69**, 2058 (1992).
- [19] R. Shyam, K. Bennaceur, J. Okołowicz, M. Płoszajczak, Preprint GANIL 99/18; *Nucl. Phys.* (2000), in print.
- [20] F.C. Barker, *Aust. J. Phys.* **33**, 177 (1980).
- [21] G. Baur, C.A. Bertulani, H. Rebel, *Nucl. Phys.* **A458**, 188 (1986).
- [22] A.N.F. Alexio, C.A. Bertulani, *Nucl. Phys.* **A505**, 448 (1989).
- [23] F. Boué, Ph.D. Thesis, University of Bordeaux 1, Centre d'Etudes Nucléaires de Bordeaux - Gradignan, Report C.E.N.B.G. 99-03; N. Iwasa *et al.*, *Phys. Rev. Lett.* **83**, 2910 (1999).
- [24] T. Motobayashi *et al.*, *Phys. Rev. Lett.* **73**, 2680 (1994); T. Kikuchi *et al.*, *Phys. Lett.* **B391**, 261 (1997).
- [25] K. Langanke, *Acta Phys. Pol.* **B31**, 281 (2000).
- [26] S.E. Woosley, D.H. Hartmann, R.D. Hoffman, W.C. Haxton, *Astrophys. J.* **356**, 272 (1990).
- [27] V.V. Balashov, A.N. Boyarkina, I. Rotter, *Nucl. Phys.* **59**, 414 (1964).